



Grant agreement no. 243964

QWeCI

Quantifying Weather and Climate Impacts on Health in Developing Countries

D3.2b Report on the advantages in terms of forecast quality of the combination of dynamical and statistical models of interannual and decadal variability for Africa

Start date of project: 1st February 2010

Duration: 42 months

Lead contractor: IC3
Coordinator of deliverable: IC3
Evolution of deliverable

Due date : M30
Date of first draft : M30
Start of review : 11 January 2013
Deliverable accepted : 22 April 2013

Project co-funded by the European Commission within the Seventh Framework Programme (2007-2013)		
Dissemination Level		
PU	Public	
PP	Restricted to other programme participants (including the Commission Services)	
RE	Restricted to a group specified by the consortium (including the Commission Services)	RE
CO	Confidential, only for members of the consortium (including the Commission Services)	



Grant agreement no. 243964

QWeCI

Quantifying Weather and Climate Impacts on Health in Developing Countries

Deliverable 3.2.b

“Report on the advantages in terms of forecast quality of the combination of dynamical and statistical models of interannual and decadal variability for Africa”

Start date of project: 1st February 2010

Duration: 42 months

Lead contractor :

Coordinator of deliverable :

Evolution of deliverable

IC3, Barcelona (Spain)

Due date :

M30 (Oct-2012)

Date of first draft :

M30 (Oct-2012)

Start of review :

Deliverable accepted :

Project co-funded by the European Commission within the Seventh Framework Programme (2007-2013)		
Dissemination Level		
PU	Public	
PP	Restricted to other programme participants (including the Commission Services)	
RE	Restricted to a group specified by the consortium (including the Commission Services)	X
CO	Confidential, only for members of the consortium (including the Commission Services)	

Report on the advantages in terms of forecast quality of the combination of dynamical and statistical models of interannual and decadal variability for Africa

L.R.L. Rodrigues, J. García-Serrano, I. Andreu-Burillo, F.J. Doblas-Reyes

The main objective of this Deliverable is the assessment of the relative advantages of combining information from different interannual forecast systems, including both dynamical and statistical systems. The combination in a single probabilistic prediction of the climate information from different systems allows the users to avoid the common problem of handling predictions with different characteristics. The problem and solutions proposed will be illustrated with annual predictions of precipitation over West Africa.

1. Introduction

Climate prediction is motivated by the evidence that current global climate models (GCMs) can, to a certain degree, capture the evolution of slow variations of the climate system when they are adequately initialised. In particular, the thermal inertia and assumed predictability of the sea surface temperatures (SSTs) imply that reliable seasonal predictions in the tropics are an achievable aim (Tompkins and Feudale 2010).

The tropical Atlantic rainfall variability over West Africa is largely dominated by, and seasonally locked to, the summertime West African monsoon (WAM), which is tightly controlled by the inter-tropical convergence zone (ITCZ) latitudinal variability and the distribution of trade winds. The WAM is sensitive to both local forcing and remote influences (e.g. Folland et al. 1986; Fontaine and Janicot 1996; Fontaine et al. 1998). The WAM variability spans a wide range of timescales, from intraseasonal (e.g. Sultan et al. 2003) to interdecadal (e.g. Janicot et al. 2001). The interannual variability of the WAM is represented by changes in precipitation over coastal regions of the Gulf of Guinea, for which the Equatorial Atlantic SST variability or Atlantic Niño is the main oceanic forcing (Janicot et al. 1998, Vizy and Cook 2001; Okumura and Xie 2004; Losada et al. 2010). The decadal variability of the WAM is well captured by low-frequency rainfall fluctuations over the semi-arid African Sahel, the southern edge of the Sahara (Folland et al. 1986; Nicholson 1993; Fontaine et al. 1995). The Sahelian rainfall variability is related to contrasting patterns of SST anomalies on a near-global scale, projecting onto an inter-hemispheric signature (Folland et al. 1986; Palmer 1986; Rowell et al. 1995; Fontaine et al. 1998). As part of this inter-hemispheric SST pattern, the main oceanic forcings of the Sahel precipitation are the Indian Ocean decadal variability (Giannini et al. 2003, 2005; Bader and Latif 2003), the Atlantic multi-decadal oscillation, or AMO (Hoerling et al. 2006; Mohino et al. 2011), and the Pacific decadal oscillation or the basin-wide inter-decadal Pacific oscillation, or IPO (Joly 2008; Mohino et al. 2011).

The WAM is a complex system with three main interacting components, namely atmosphere, land and ocean, whose different inertias generate complex interactions. A clear example is the latitudinal jump of the ITCZ-related rainbelt, whereby the Sahelian rainy season occurs in July-September and varies in intensity both at interannual and decadal timescales (e.g. Fontaine et al. 1998; Janicot et al. 1998; Sultan and Janicot 2000). The physical mechanisms driving WAM dynamics have been the subject of numerous diagnostics studies during the recent decades. However, prediction of the seasonal rainfall over West Africa still remains one of the major concerns for the local population, because of its impact on agriculture, health and water supply, and consequently on the economy of its integrating countries. One of the objectives of this Deliverable aims to assess the maximum lead time for which forecasts of the WAM rainfall at the intraseasonal-to-annual range in current climate prediction systems.

The Guinean precipitation and the Sahelian rainfall account for most of the SST-forced WAM variability at seasonal-to-decadal timescales. When climate models are forced with observed SSTs, they successfully reproduce the observed interannual-Guinean and decadal-Sahelian rainfall

variabilities (Giannini et al. 2003, 2005; Moron et al. 2003; Tippet and Giannini 2006). Thus, the SST forcing can be considered as the dominant driver of the WAM rainfall variability. However, the WAM forecast skill in coupled models becomes a serious trouble. This is particularly true for predicting the interannual-to-decadal variability (Joly et al. 2007; Joly and Voltaire 2009a, 2009b; García-Serrano et al. 2012). Nonetheless, Batté and Déqué (2011), using the ENSEMBLES Stream-2 seasonal re-forecasts, pointed out the additional skill in GCMs when compared to climatology for a variable highly dependent on parameterizations such as precipitation. These results are encouraging and contrast with the reputation coupled forecast systems have been given over the years when it comes to precipitation forecasts outside the tropical Pacific basin. Unfortunately, this does not translate into skill in predicting the dominant WAM rainfall regimes. Perhaps, the exception is the Guinean precipitation, for which there exists a maximum (up to date) forecast correlation with the observations of ~0.5-0.6 using direct model output of rainfall. The Sahelian precipitation, instead, remains a clear hurdle for coupled GCMs. Bouali et al. (2008), by using the DEMETER seasonal re-forecasts, found a correlation of 0.16 with raw rainfall data, while the model-output-statistics (MOS) calibration with atmospheric dynamics and moist static energy fluxes did not lead to better results. Maybe as evidence of the improvement in both models and ocean analysis, the skill at predicting summer monsoon rainfall anomalies has increased a bit in recent years. Thus, Philippon et al. (2010), using the ENSEMBLES Stream-1 seasonal re-forecasts, improved the Sahelian precipitation forecasts from a correlation of 0.17 with the direct model output to 0.51 with a MOS calibration, which included five atmospheric fields. Likewise, and in an operational seasonal prediction context, Tompkins and Feudale (2010) found a forecast correlation of the Sahelian rainfall of around ~0.4 using the ECMWF System3 re-forecasts. This Deliverable updates the forecast quality and reproducibility of the dominant WAM rainfall regimes (Guinean and Sahelian) by evaluating the most recent operational seasonal prediction systems, namely ECMWF's System4¹ (hereafter SYST4) and a statistical forecast system based on linear regression, as well as their combinations. This Deliverable uses an innovative approach to analyze the intraseasonal evolution of the WAM precipitation based on the assessment of the ability of these forecast systems in simulating and predicting the timing of the latitudinal migration of the tropical convection.

2. Interannual forecast systems

This Deliverable uses data from the most recent operational climate forecast system of the European Centre for Medium-Range Weather Forecasts (ECMWF), SYST4, and a simple statistical model based on lagged regression. The project uses sets of retrospective forecasts (re-forecasts or hindcasts) over a recent period produced by SYST4. The SYST4 re-forecasts have 15 members for all start dates (Feb, May, Aug, Nov), and cover the 29 years from 1982 to 2010. The length of these integrations is thirteen months. The long time period in the hindcasts allows reliable calibration of the forecasts and good assessment of their skill.

The statistical model used, which is probabilistic in nature, follows the statistical model used in Coelho et al. (2004), except that the predictor and the predictand are two different climate variables. The predictand is the WAM precipitation while the predictors are two climate indices. The two climate indices are the Niño3.4 index, which was used to predict the Guinean precipitation, and the AMO, which was used to predict the Sahelian precipitation. The statistical model was built in one-year out cross-validation mode for the target years 1982-2010 and the predictors are three-month averages of the two above mentioned climate indices. For example, to forecast the Guinean precipitation during the summer WAM season 1982 with lead time zero, a least-squared simple linear regression of the Guinean precipitation (i.e. May through November) on the three-month averaged Niño3.4 index of February, March and April was performed using the training period 1983-2010. To forecast the summer WAM season 1983, the years 1982 and 1984-2010 were used

1 <http://www.ecmwf.int/products/changes/system4/>

as the training period.

3. The Forecast Assimilation method

The forecast assimilation (FA) is a Bayesian method for calibrating and combining predictions from several sources using prior (historical) empirical information (Stephenson et al. 2005). It has been used to combine the SYST4 with the statistical model hindcasts. In one case, the statistical model predictions were combined with the ones by SYST4 having a climatological forecast as the prior information (FAC). In a second approach, the FA method was used employing the SYST4 hindcasts as the likelihood and the statistical model predictions as the prior information (FAS).

4. Forecast quality assessment

The forecast quality of the WAM precipitation predictions of the combinations and individual forecast systems described above was assessed from a deterministic and a probabilistic point of view. The correlation coefficient was used to assess the degree of linear association between the predicted mean and observed WAM precipitation. Several probabilistic verification scores have been computed for dichotomous events of the two leading modes of the WAM precipitation variability (i.e. the PC1 for the Guinean mode and the PC2 for the Sahelian mode) exceeding the median and the upper quartile of the climatological distribution. These thresholds were estimated using ensemble members for the predictions of the dynamical forecast systems and all available years. Separate threshold estimates were obtained for the predictions and the observations.

Two different types of hindcasts were handled in this study: ensemble predictions (SYST4) and sets of predictions defined by a forecast mean and standard deviation (those provided by the statistical model, the FAC and the FAS). For those forecast systems that did not have ensemble hindcasts, the Gaussian forecast distribution of each year was sampled with size 10,000 to obtain samples from which to compute the median and quartiles of the corresponding climatological distributions. The 10,000 sample size was chosen because it was found to provide robust estimates of the climatological probability density function (PDF). Its robustness was estimated by calculating the Brier skill score between the predicted and observed probabilities 1,000 times for the statistical model and for a given start date. These 1,000 estimations were performed with sample size 11, 51, 100, 1,000 and 10,000. The sample size 10,000 had the smallest spread in the histogram of the 1,000 estimated values of the correlation coefficient. Finally, the probability forecasts were estimated using the estimated thresholds (median and upper quartile).

The main measure of probabilistic forecast quality is the Brier score (BS), which can be defined as:

$$BS = \frac{1}{N} \sum_{i=1}^N (p_i - o_i)^2 \quad (1)$$

where p_i is the probability forecast and o_i is the observation, which is set to be one if the event happened and 0 if it did not happen, for the i th year. The BS could be generalized in the form of a skill score where the forecast of a given system is compared to a reference prediction system, which is usually a much simpler forecast such as the climatological frequency of the event. This generalization is called the Brier skill score (BSS), and could be written as $BSS = 1 - \frac{BS}{BS_c}$, where

BS is the Brier score of a given system and BS_c is the Brier score of the reference forecast. Positive BSS means the BS of the system is better than the BS of the reference forecast.

Other forecast quality attributes have also been analyzed, among them the reliability and resolution components of the BS (Mason and Stephenson 2008). The reliability component of the BS verifies the degree of correspondence between the frequency of events predicted by the system and the frequency of events that actually happened and measures the degree of trustworthiness of the predicted probabilities. The resolution, on the other hand, measures the ability of the forecasts to

distinguish events that have forecast probabilities different from the climatological frequency. A third component of the BS is the uncertainty, which is associated with the uncertainty of the observations for a given event and does not depend on the predictions.

These three components of the BS are estimated by stratifying the forecast probabilities into a set of bins, the number of which is usually smaller than the number of possible forecast probabilities. However, depending on the number of bins used to stratify the forecast probabilities, the sum of the three components does not equal the BS computed using equation (1). Two additional components that account for the within-bin variance of the forecasts and the within-bin covariance between forecasts and observations are also needed to make the components of the BS less sensitive to the number of bins (Stephenson et al. 2008). These two extra components were added to the resolution component of the BS to make a generalized resolution term.

It has been shown that the standard decomposition of the BS is biased, being the reliability component positively biased, the uncertainty negatively biased, and the resolution either negatively or positively biased (Ferro and Fricker 2012). A new estimate of the less-biased reliability, generalized resolution, and the uncertainty components of the BS by Ferro and Fricker (2012) will be used in this study. The skill scores of the less-biased reliability and generalized resolution were computed as follows (Doblas-Reyes et al. 2005):

$$BSS_{REL} = 1 - \frac{BS_{REL}}{BS_{UNC}} \quad (2)$$

$$BSS_{GRES} = \frac{BS_{GRES}}{BS_{UNC}} \quad (3)$$

where BS_{REL} is the less-biased reliability component of the BS, BS_{GRES} is the less-biased generalized component of the BS, and BS_{UNC} is the bias-free uncertainty component of the BS.

5. Results

The skill and reproducibility of the latitudinal migration of the ITCZ is examined by means of Hovmöller diagrams, in which the precipitation is longitudinally averaged as shown in Fig. 1 for West Africa (10°W-10°E). Also shown in Fig. 1 is the spatial distribution of precipitation climatology in GPCP, which corresponds to the observational reference dataset, during boreal summer (July-September; JAS), the main rainy season. JAS represents the central months in the corresponding latitude-time Hovmöller diagrams analyzed, which span May throughout November for West Africa. The target period of study for the Hovmöller diagrams is 1982-2010. The latitudinal window of the Hovmöller diagram in each case is EQ-20°N.

Monthly precipitation anomalies in these latitude-time diagrams are obtained by subtracting the corresponding monthly climatology. In that way, each month in the time dimension of the Hovmöller diagram involves interannual variability. Note that neither detrending nor filtering has been applied to the data. After, a principal component analysis (PCA/EOF; von Storch and Zwiers 2001) is performed upon these longitudinally-averaged precipitation anomalies. In this case, PCA provides a set of latitude-time patterns (empirical orthogonal functions, EOFs) and associated standardized time series (principal components, PCs; Fig. 2). The information associated with each PCA mode is completed by the corresponding fraction of explained variance. The PCA results have been described in terms of correlation maps, obtained by correlating the anomaly time series for surface temperature in different seasons with the PC related to each mode. Note that according to this PCA set-up, the leading EOFs correspond to the dominant interannual variability modes of the intra-seasonal evolution of precipitation. These EOFs were widely described in the deliverable D3.2.a, while here a summary is presented and additional results shown.

The systematic error of SYST4 in tropical convection is tightly associated with the warming drift in

the tropical Atlantic SSTs (4°S - 4°N / 15°W - 10°E ; Fig. 2 of D3.2.a, top right), which is a well-known problem in coupled GCMs leading to a southward shift of the local ITCZ and a failure to reproduce the Atlantic equatorial cold tongue (e.g. Richter and Xie 2008). Figure 2 of D3.2.a shows how as the lead time for the Hovmöller diagram increases, that is when using predictions for the start dates from May to the previous November, the SST warming drift in the boreal summer months is higher and, hence, rainfall biases are larger as well. The dipole-like pattern of the rainfall mean error reflects the wrong latitudinal position of the model ITCZ, which involves more rain than observed at equatorial latitudes and a clear deficit along the Sahelian belt ($\sim 10^{\circ}\text{N}$ - 18°N). Note also how SYST4 lengthens the WAM pre-onset stage, yielding a surplus of precipitation in July (one month later than observed).

The observed interannual variability of the longitudinally-averaged precipitation in West Africa is dominated by the Guinean (EOF1, 27%; Fig. 3 of D3.2.a) and Sahelian (EOF2, 20%; Fig. 4 of D3.2.a) rainfall regimes. The former reflects changes in convection strength within the ITCZ during the pre-onset months (first rainy season in the Gulf of Guinea; e.g. Fontaine et al. 2008), and is associated with the recent Atlantic-Pacific inter-tropical connection (e.g. Rodríguez-Fonseca et al. 2009). The latter shows a dipolar pattern with maximum amplitude over 10°N - 18°N , which reflects more/less northward penetration of the rainbelt and projects onto the inter-hemispheric SST gradient (AMO, IPO). Note the AMO-related surface temperatures in the eastern Mediterranean basin and the positive correlations over the Saharan heat low area during JAS, which have been shown to strongly contribute regulating the Sahelian precipitation (Haarsma et al. 2005; Biasutti et al. 2008; Fontaine et al. 2010). The time-series of the principal components associated with these EOFs are shown in Fig. 2 (thick black). The Guinean rainfall regime (PC1; left) is largely dominated by interannual variability. By contrast, the Sahelian rainfall regime (PC2; right) encompasses a lower-frequency fluctuation that projects onto a positive trend, which actually corresponds to the partial recovery after the Sahel drought in the 1980s (e.g. Mohino et al. 2011).

The leading EOF mode of the longitudinally-averaged precipitation in SYST4 at each start date is the Guinean rainfall regime (Figs. 3,5 of D3.2.a), which accounts for 30%, 38%, and 39% of the total precipitation variance with predictions from the May, February, and November start dates, respectively. These fractions of variance in SYST4 overestimate that in GPCP. As the lead time for the Hovmöller diagram increases, successive EOF patterns reflect the model systematic error in tropical precipitation, where the Guinean precipitation increases in the model at the expense of the precipitation over the Sahel (cf. Figs. 3, 5 and Fig. 2 in D.3.2.a). The Guinean precipitation modes capture the recent Atlantic-Pacific inter-tropical relationship. At each start date, the correlation maps of surface temperature suggest that SYST4 delays the peak of the Atlantic Niño with respect to the observations, occurring in JAS instead of MJ (Polo et al. 2008; Losada et al. 2010). This finding might be related to the systematic error described above (Fig. 2 of D.3.2.a) where the model delays the WAM pre-onset. The time series of these EOFs for the start dates ranging from May (Fig. 2, top-left) to November (Fig. 2, bottom-left) show how the spread of the ensemble grows, and the accuracy in recapturing the observed PC decreases, as the lead time increases.

The second EOF of the longitudinally-averaged precipitation in SYST4 is the Sahelian rainfall regime (Figs. 4, 6 of D.3.2.a), which accounts for 11%, 10%, and 10% of the total precipitation variance for the May, February, and November start dates, respectively. These fractions of variance underestimate the fractions of variance obtained with GPCP. For all start dates the simulated Sahelian mode shows a dipole-like pattern between the coastal regions and 10°N - 15°N . As also shown in the observations, the heart of the simulated Sahelian rainfall occurs in August. The correlation maps of surface temperature project onto the inter-hemispheric gradient that includes the AMO and IPO signatures, while no clear relationship appears with the Indian Ocean temperatures. Despite the spread growing with lead time (Fig. 2, right), the principal components of these EOFs show an apparent positive trend that mimics the observed evolution, with negative (positive)

anomalies before (after) late 1990s.

Figure 3 shows the anomaly forecasts of the Guinean rainfall regime (first EOF mode; PC1) for the Statistical model, SYST4, FAC and FAS for the period 1982-2010. Forecasts are for the start date of May (lead zero). As for the statistical model, the predictor is the three-month average of February, March and April. Given that our target period is the months between May and November, as described above, the three-month average of February, March and April would be the last available as a predictor. The one-year-out cross-validation method was used to estimate the regression coefficients of the statistical model. This means that to forecast the Guinean rainfall regime (PC1) for the year 1982, firstly the GPCP PC1 for the period 1983-2010 were regressed on the three-month average of February, March and April for the same period to estimate the regression coefficients. Then, the three-month average of February, March and April of 1982 was used as a predictor to forecast the PC1 of 1982.

The black line represents the observational reference from GPCP, the red line is the predicted mean anomaly of the individual forecast systems and the combinations, and the grey band is the 95% prediction interval for each forecast system, given by the predicted mean anomaly plus or minus 1.96 times the predicted standard deviation. The mean prediction of the statistical model underestimates the interannual variability of the Guinean rainfall regime and the linear correspondence between the statistical model predictions and the observations is 0.29. On the other hand, SYST4 is able to simulate well the interannual variability and, except for the 1988 positive rainfall anomaly and the 2005 extreme drought event, its predictions have a high degree of linear correspondence with the observations (correlation=0.77). Both combinations resemble SYST4's predictions, which means that for this specific region and start date the statistical model received little weight in the combination procedure. None of the forecast systems were able to represent properly in their predicted interval the 2005 extreme drought event. However, the statistical model predicted interval was able to predict the 1988 positive rainfall anomaly. All forecast systems have, for this specific region and start date, a high reliability skill score and low resolution skill score. Thus, the BSS for both probabilistic events analyzed here (anomalies above the median and upper quartile) is low, and even zero for the statistical model. In this case, no improvement was achieved when combining SYST4 with the statistical model, which is something expected given the low skill of the statistical model.

The Sahelian rainfall regime (second EOF mode; PC2) predictions for the start date of November are displayed in Figure 4. As in the previous case of the Guinean rainfall regime, the statistical model underestimates the interannual variability; however, as pointed out above, the Sahelian rainfall regime encompasses more of a lower-frequency variability with a positive trend. Because the statistical model is able to reproduce part of this linear trend it has a correlation of 0.36, similar to the correlation of SYST4 (0.37). The single forecast systems predicted interval is able to represent the observed PC2, except for the statistical model in the year 1994. In this case, the inclusion of the statistical model as the prior information (FAS) helps improve the accuracy (i.e. correlation) of the prediction when compared to both single forecast systems. However, all forecast systems have a high reliability and a low resolution which resembles a climatological forecast and that is one of the reasons why the probabilistic skill scores are close to zero.

Ensemble-mean anomaly correlation coefficients between the longitudinally-averaged precipitation modes in GPCP and SYST4 showed skilful results (Fig. 7 of D3.2.a, and Figs. 5, 6). The Guinean rainfall (leading EOF) skill is statistically significant with a lead time of up to three months, with ~0.8 for the May start date (zero lead time) and ~0.5 for the February start date. The sharp decrease in the prediction skill of the Guinean rainfall appears to be consistent with the progressive lack of skill in forecasting the evolution of the cold tongue in the equatorial Atlantic as the lead time for May-June increases, as revealed in Section 3.1 of D3.2.a. This is also in agreement with the skill

decay in forecasting precipitation anomalies over maritime regions of the Gulf of Guinea (Section 3.1 of D.3.2.a). The Sahelian mode (second EOF) has statistically significant skill only for the start date of May (zero lead time) with a correlation above 0.6, while for the February start date is ~ 0.45 (0.38 in Fig. 6 as the target period is slightly different). Nevertheless, it is worth noting that SYST4 yield positive correlations for both Hovmöller-based rainfall modes at the three start dates considered. Especially noticeable is the score above 0.3 (0.37 in Figs. 4, 6, when using the most updated dataset) in the Sahelian precipitation for the November start date. Actually, the mild decrease in the prediction skill of the Sahelian rainfall (Fig. 7 of D.3.2.a) could be consistent with the good performance in forecasting surface temperatures over the eastern Mediterranean basin and the Sahara heat low region during the target period July-to-September, as shown in Section 3.1 of D.3.2.a. Likewise, these results seem to be in agreement with the positive correlations found for the Sudan-Sahel belt precipitation from the three start dates considered here (Section 3.1 of D.3.2.a).

The deterministic skill of the statistical model shows a different pattern when compared to those of the SYST4. First of all, the statistical model predictions have lower skill than the ones by SYST4 for all six cases analyzed here (i.e. two rainfall regimes and three start dates). Secondly, the decreasing skill with increasing lead time of the Guinean rainfall is less strong in the statistical model when compared to SYST4. However, for the leads zero and three months, SYST4 has much better predictions when compared to the statistical model. Thirdly, the statistical model has higher skill for longer leads when predicting the Sahelian precipitation. This could be explained by the fact that the predictors for the lead six months (AMO of the three-month average of August, September and October) have stronger trend than the lead zero months (AMO of the three-month average of February, March and April) (not shown).

The combination of SYST4 with the statistical model does not improve the Guinean rainfall regime deterministic forecasts. This could be explained by the fact that the statistical model has low skill of its mean predictions. However, when the statistical model has comparable skill compared to the SYST4, as in the case for the Sahelian rainfall regime with lead time six (Fig. 4), the addition of the statistical model predictions as a prior information contributes to an increased deterministic skill of the combined predictions.

The probabilistic scores are comparable to those of a climatological forecast (Figs. 5, 6) except for the lead-zero predictions in both analyzed rainfall regimes. That is, the single forecast systems and combinations have high reliability and low resolution. For lead time zero, in both analyzed rainfall regimes, the combination method that included the statistical model in the likelihood function having the climatology forecast as the prior (i.e. FAC) has the best probabilistic predictions. However, because the statistical model in both regimes has zero resolution skill score it could be argued that the improvement in the probabilistic forecast in terms of BSS for both events (above the median and the upper quartile) came from the calibration of the SYST4 rather than from the inclusion of the statistical model. The benefits of calibration to increase predictions skill in the tropics have been shown in previous studies (e.g. Doblus-Reyes et al. 2005).

6. Conclusions

This deliverable dealt with the assessment of the relative advantages of combining information from different interannual forecast systems, including both dynamical and statistical systems. The forecast quality assessment was performed for the longitudinally-averaged precipitation over West Africa (10°W-10°E). The two leading modes of precipitation variability for this region are: the Guinean and the Sahelian rainfall regimes. A simple statistical model based on lagged regression was combined with SYST4 to assess the relative merits of this combination. The Forecast Assimilation method was used for the combination.

It is shown that SYST4 has good deterministic skill when predicting the Guinean and the Sahelian

rainfall regimes for the start dates of May and February. On the other hand, the statistical model has low correlation when predicting these two rainfall regimes, and the only occasion when it has correlation above 0.3 is when predicting the Sahelian regime with start date in November. Therefore, combining these two forecast systems did not take to improved forecast.

Both forecast systems have probabilistic prediction skill comparable to that of a climatological forecast; that is, having high reliability skill score and low resolution skill score. On the other hand, when combining the SYST4 with the statistical model having the climatology as the prior a slightly improvement in terms of BSS is observed for the start date of May (lead zero) in both rainfall regimes. However, this could be a result of the calibration of the SYST4 rather than the inclusion of the information from the statistical model, given that the latter had a high reliability and low resolution.

Further investigation is needed to assess whether the inclusion of other dynamical forecast systems or the combination of SYST4 with a better statistical model could make a better forecast.

Acknowledgements

GPCP Precipitation data was provided by the NOAA/OAR/ESRL PSD, Boulder, Colorado, USA, from their Web site at <http://www.esrl.noaa.gov/psd/>. We would also like to acknowledge NOAA ESRL for the ERSST data.

References

Bader, J., M. Latif (2003): The impact of decadal-scale Indian Ocean sea surface temperature anomalies on Sahelian rainfall and the North Atlantic Oscillation. *Geophys. Res. Lett.*, 30, 2169, doi 10.1029/2003GL018426.

Batté, L., M. Déqué (2011): Seasonal predictions of precipitation over Africa using coupled ocean-atmosphere general circulation models: skill of the ENSEMBLES project multimodel ensemble forecasts. *Tellus A*, 63.

Biasutti, M., I. M. Held, A. H. Sobel, A. Giannini (2008): SST forcings and Sahel rainfall variability in simulations of the twentieth and twenty-first centuries. *J. Clim.*, 21, 3471-3486.

Bouali, L., N. Philippon, B. Fontaine, J. Lemond (2008): Performance of DEMETER calibration for rainfall forecasting purposes: application to the July-August Sahelian rainfall. *J. Geophys. Res.*, 113, D15111.

Coelho, C. A. S., S. Pezzulli, M. Balmaseda, F. J. Doblas-Reyes, D. B. Stephenson (2004): Forecast calibration and combination: A simple Bayesian approach for ENSO. *J. Clim.*, 17, 1504-1516.

Doblas-Reyes, F. J., R. Hagedorn, T. N. Palmer (2005): The rationale behind the success of multi-model ensembles in seasonal forecasting - II. Calibration and combination. *Tellus A*, 57, 234-252.

Ferro, C. A. T., T. E. Fricker (2012): A bias-corrected decomposition of the Brier score. *Q. J. R. Meteor. Soc.*, doi: 10.1002/qj.1924.

Folland, C. K., T. N. Palmer, D. E. Parher (1986): Sahel rainfall and worldwide sea surface temperature. *Nature*, 320, 602-607.

Fontaine, B., S. Janicot, V. Moron (1995): Rainfall anomaly patterns and wind field signals over West Africa in August (1958-1989). *J. Clim.*, 8, 1503-1510.

Fontaine, B., S. Janicot (1996): Near-global sea surface temperature variability associated with West African rainfall anomaly types. *J. Clim.*, 9, 2935-2940.

- Fontaine, B., S. Trzaska, S. Janicot (1998): Evolution of the relationship between near global and Atlantic SST modes and the rainy season in West Africa: statistical analyses and sensitivity experiments. *Clim. Dyn.*, 14, 353-368.
- Fontaine, B., S. Louvet, P. Roucou (2008): Definition and predictability of an OLR-based West African monsoon onset. *Int. J. Climatol.*, 28, 1787-1798.
- Fontaine, B., J. García-Serrano, P. Roucou, B. Rodríguez-Fonseca, T. Losada, F. Chauvin, S. Gervois, S. Sijikumar, P. Ruti, S. Janicot (2010): Impacts of warm and cold situations in the Mediterranean basins on the West African monsoon: observed connection patterns (1979-2006) and climate simulations. *Clim. Dyn.*, 35, 95-114.
- García-Serrano, J., F. J. Doblas-Reyes, R. J. Haarsma, I. Polo (2012): Decadal prediction of the West African monsoon. *J. Geophys. Res.* (under review).
- Giannini, A., R. Saravanan, P. Chang (2003): Oceanic forcing of Sahel rainfall on interannual to interdecadal timescales. *Science*, 302, 1027-1030.
- Giannini, A., R. Saravanan, P. Chang (2005): Dynamics of the boreal summer African monsoon in the NSIPP1 atmospheric model. *Clim. Dyn.*, 25, 517-535.
- Haarsma, R. J., F. M. Selten, S. L. Weber, M. Kliphuis (2005): Sahel rainfall variability and response to greenhouse warming. *Geophys. Res. Lett.*, 32, L17702, doi:10.1029/2005GL023232.
- Hoerling, M., J. Hurrell, J. Eischeid, A. Phillips (2006): Detection and attribution of twentieth-century Northern and Southern African rainfall change. *J. Clim.*, 19, 3989-4008.
- Janicot, S., A. Harzallah, B. Fontaine, V. Moron (1998): West African monsoon dynamics and eastern equatorial Atlantic and Pacific SST anomalies. *J. Clim.*, 11, 1874-1882.
- Janicot, S., S. Trzaska, I. Pocard (2001): Summer Sahel-ENSO teleconnection and decadal time scale SST variations. *Clim. Dyn.*, 18, 303-320.
- Joly, M., A. Voltaire, H. Douville, P. Terray, J.-F. Royer (2007): African monsoon teleconnections with tropical SSTs: validation and evolution in a set of IPCC4 simulations. *Clim. Dyn.*, 29, 1-20.
- Joly, M (2008): Rôle des océans dans la variabilité climatique de la Mousson Africaine. PhD Dissertation, Université Paris-Est.
- Joly, M., A. Voltaire (2009a): Influence of ENSO on the West African monsoon: temporal aspects and atmospheric processes. *J. Clim.*, 22, 3193-3210.
- Joly, M., A. Voltaire (2009b): Role of the Gulf of Guinea in the inter-annual variability of the West African monsoon: what do we learn from CMIP3 coupled simulations?. *Int. J. Climatol.*, doi 10.1002/joc.2026.
- Losada, T., B. Rodríguez-Fonseca, S. Janicot, S. Gervois, F. Chauvin, P. Ruti (2010): A multi-model approach to the Atlantic equatorial mode: impact on the West African monsoon. *Clim. Dyn.*, 35, 29-43.
- Mason, S. J., D. B. Stephenson (2008): How can we know whether the forecasts are any good? In: Troccoli A, Harrison MSJ, Anderson DLT, Mason SJ (Ed) Seasonal Climate Variability: Forecasting and Managing Risk, Springer Academic Publishers, Dordrecht, pp 259-289.
- Mohino, E., S. Janicot, J. Bader (2011): Sahelian rainfall and decadal to multidecadal SST variability. *Clim. Dyn.*, 37, 419-440.
- Moron, V., N. Philippon, B. Fontaine (2003): Skill of Sahel rainfall variability in four atmospheric GCMs

- forced by prescribed SST. *Geophys. Res. Lett.*, 30, 2221, doi 10.1029/2003GL018006.
- Nicholson, S. E. (1993): An overview of African rainfall fluctuations of the last decade. *J. Clim.*, 6, 1463-1466.
- Okumura, Y., S.-P. Xie (2004): Interaction of the Atlantic equatorial cold tongue and the African monsoon. *J. Clim.*, 17, 3589-3602.
- Palmer, T. N. (1986): Influence of the Atlantic, Pacific, and Indian oceans on Sahel rainfall. *Nature*, 322, 251-253.
- Philippon, N., F. J. Doblas-Reyes, P. M. Ruti (2010): Skill, reproducibility and potential predictability of the West African monsoon in coupled GCMs. *Clim. Dyn.*, 35, 53-74.
- Polo, I., B. Rodríguez-Fonseca, T. Losada, J. García-Serrano (2008): Tropical Atlantic Variability modes (1979-2001). Part I: time-evolving SST modes related to West African rainfall. *J. Clim.*, 21, 6457-6475.
- Richter, I., S.-P. Xie (2008): On the origin of the equatorial Atlantic biases in coupled general circulation models. *Clim. Dyn.*, 31, 587-598.
- Rodríguez-Fonseca, B., I. Polo, J. García-Serrano, T. Losada, E. Mohino, C. R. Mechoso, F. Kucharski (2009): Are Atlantic Niños enhancing Pacific ENSO events in recent decades?. *Geophys. Res. Lett.*, 36, L20705, doi 10.1029/2009GL040048.
- Rowell, D. P., C. K. Folland, K. Maskell, N. M. Ward (1995): Variability of summer rainfall over tropical North Africa (1906-92): observations and modelling. *Q. J. R. Meteorol. Soc.*, 121, 669-704.
- Sultan, B., S. Janicot (2000): Abrupt shift of ITCZ over West Africa and intra-seasonal variability. *Geophys. Res. Lett.*, 27, 3353-3356.
- Sultan, B., S. Janicot, A. Diedhiou (2003): The West African monsoon dynamics. Part I: documentation of intraseasonal variability. *J. Clim.*, 16, 3389-3406.
- Stephenson, D. B., C. A. S. Coelho, F. J. Doblas-Reyes, M. Balmaseda (2005): Forecast Assimilation: A unified framework for the combination of multi-model weather and climate predictions. *Tellus A*, 57, 253-264.
- Stephenson, D. B., C. A. S. Coelho, I. T. Jolliffe (2008): Two extra components in the Brier Score decomposition. *Weather Forecasting*, 23, 752-757.
- Tippet, M. K., A. Giannini (2006): Potentially predictable components of African summer rainfall in an SST-forced GCM simulation. *J. Clim.*, 19, 3133-3144.
- Tompkins, A. M., L. Feudale (2010): Seasonal ensemble predictions of West African monsoon precipitation in the ECMWF System 3 with a focus on the AMMA special observing period in 2006. *Wea. Forecasting*, 25, 768-788.
- Vizy, E. K., K. H. Cook (2001): Mechanisms by which Gulf of Guinea and eastern North Atlantic sea surface temperature anomalies can influence African rainfall. *J. Clim.*, 14, 795-821.
- von Storch, H., F. W. Zwiers (2001): Statistical analysis in climate research. Cambridge University Press, UK.

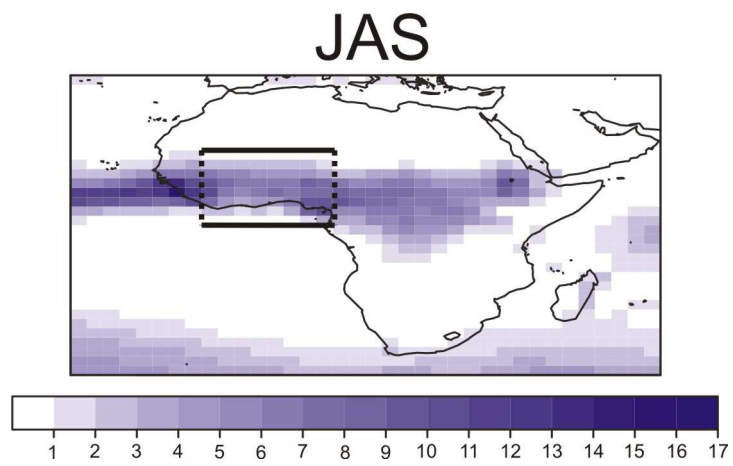


Figure 1. Spatial distribution of GPCP precipitation climatology (mm/day) over the period 1982-2008. Black box indicate the spatial domain for the Hovmöller diagram upon the West African monsoon: longitudinal-average along 10°W-10°E and latitudinal window over EQ-20°N.

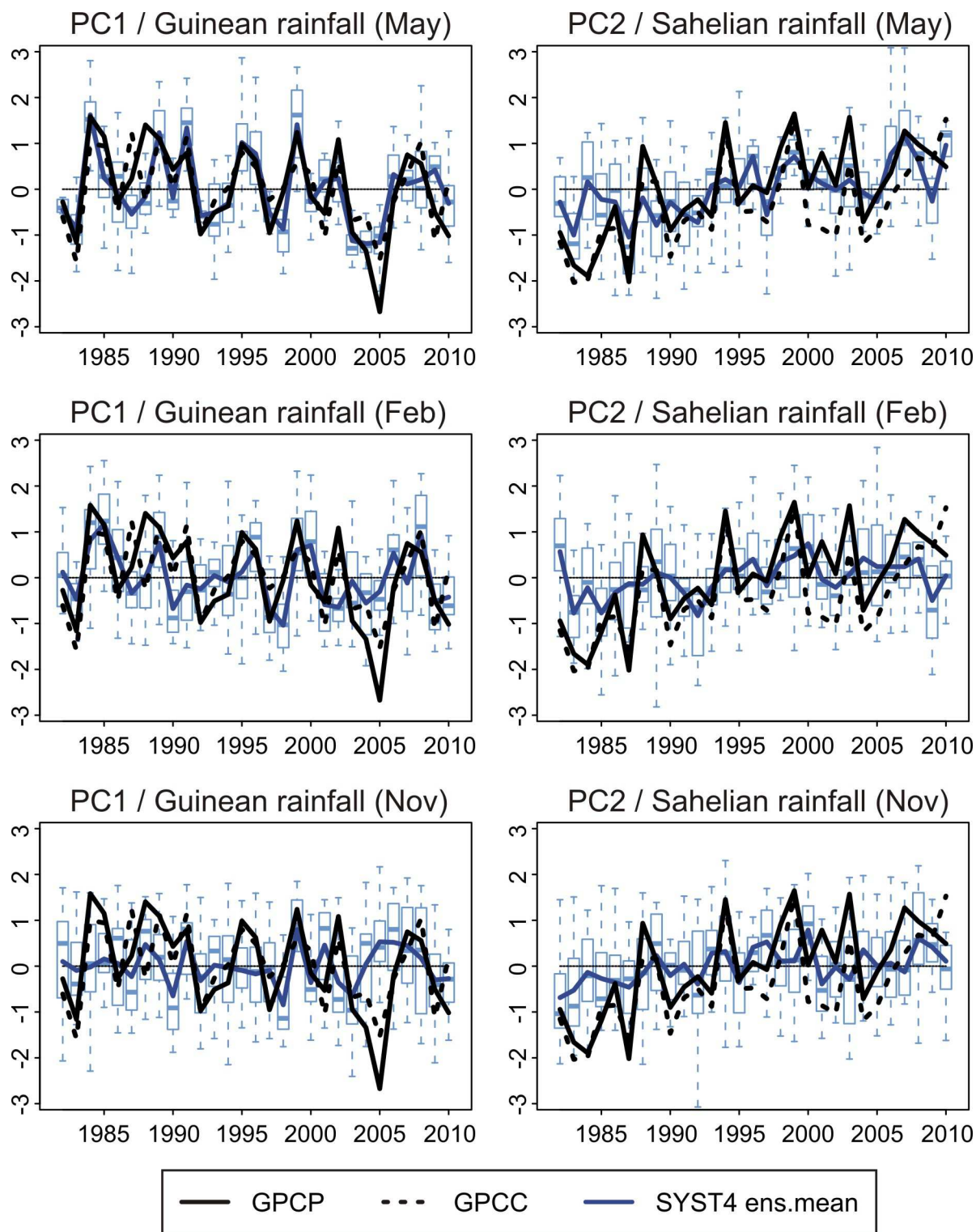


Figure 2. Standardized principal components (PCs) associated with the EOFs of Hovmöller precipitation diagram (Fig. 1) described in the Deliverable 3.2.a but over 1982-2010: GPCP (solid black), GPCP (dashed black), ensemble-mean SYST4 (solid dark blue), and box-and-whisker representation of the ensemble range in SYST4 (light blue). The Guinean rainfall regime corresponds to the first EOF mode (PC1; left column); the Sahelian rainfall regime to the second EOF mode (PC2; right column). Three start dates have been used from SYST4: May (top), February (middle) and November (bottom).

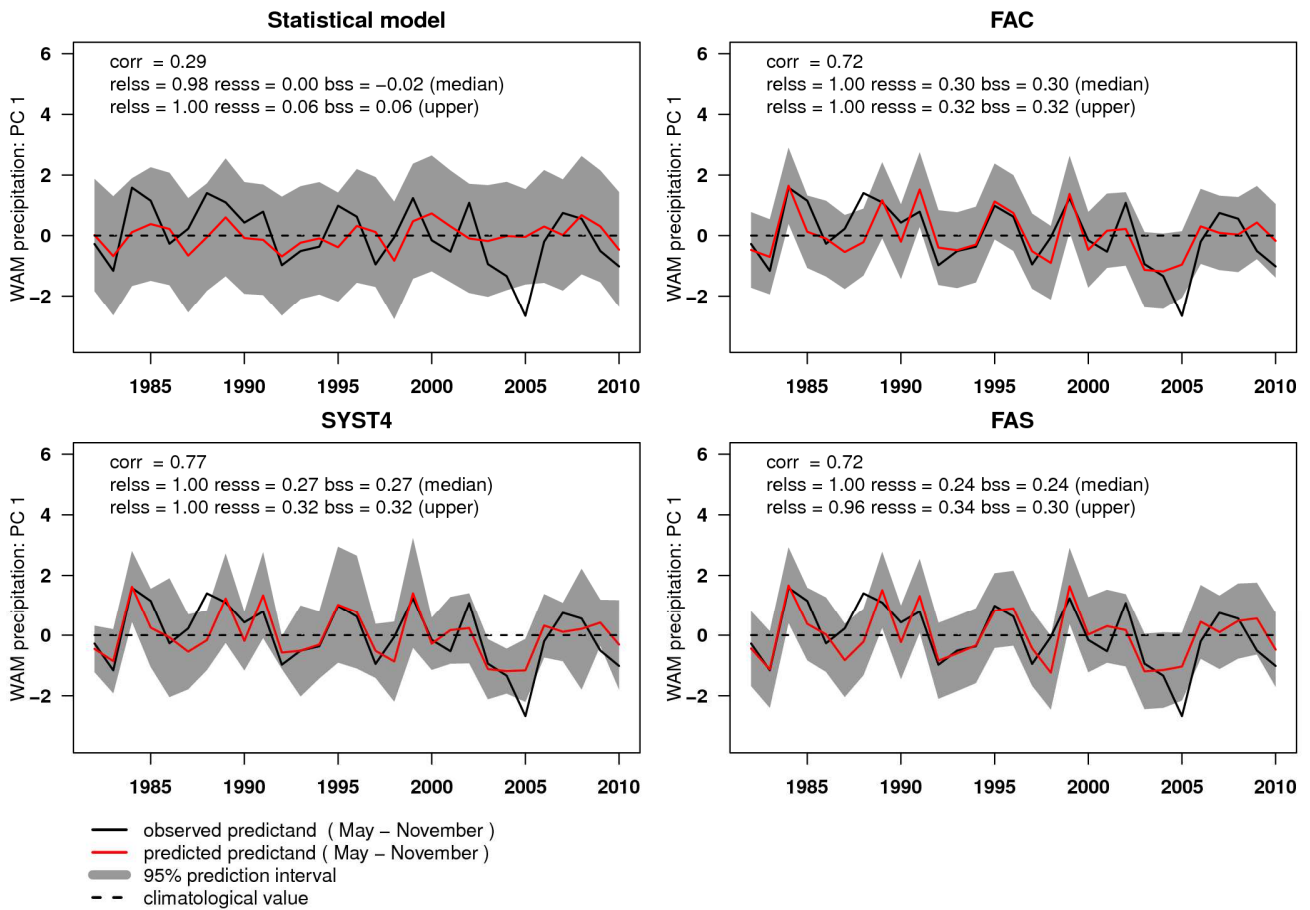


Figure 3. Monthly forecast anomalies of the Guinean rainfall regime (first EOF mode; PC1) for the Statistical model, SYST4, FAC and FAS. Forecasts are for the start date of May. Observed values (black solid line), predicted values (red solid line), 95% predicted interval (grey area) and the climatology value of May (black dashed line). Several scores are displayed in each panel: the correlation coefficient (corr), and the Brier skill score (bss) and its reliability (relss) and resolution (resss) components for dichotomous events of the PC1 anomalies exceeding the median and the upper quartile

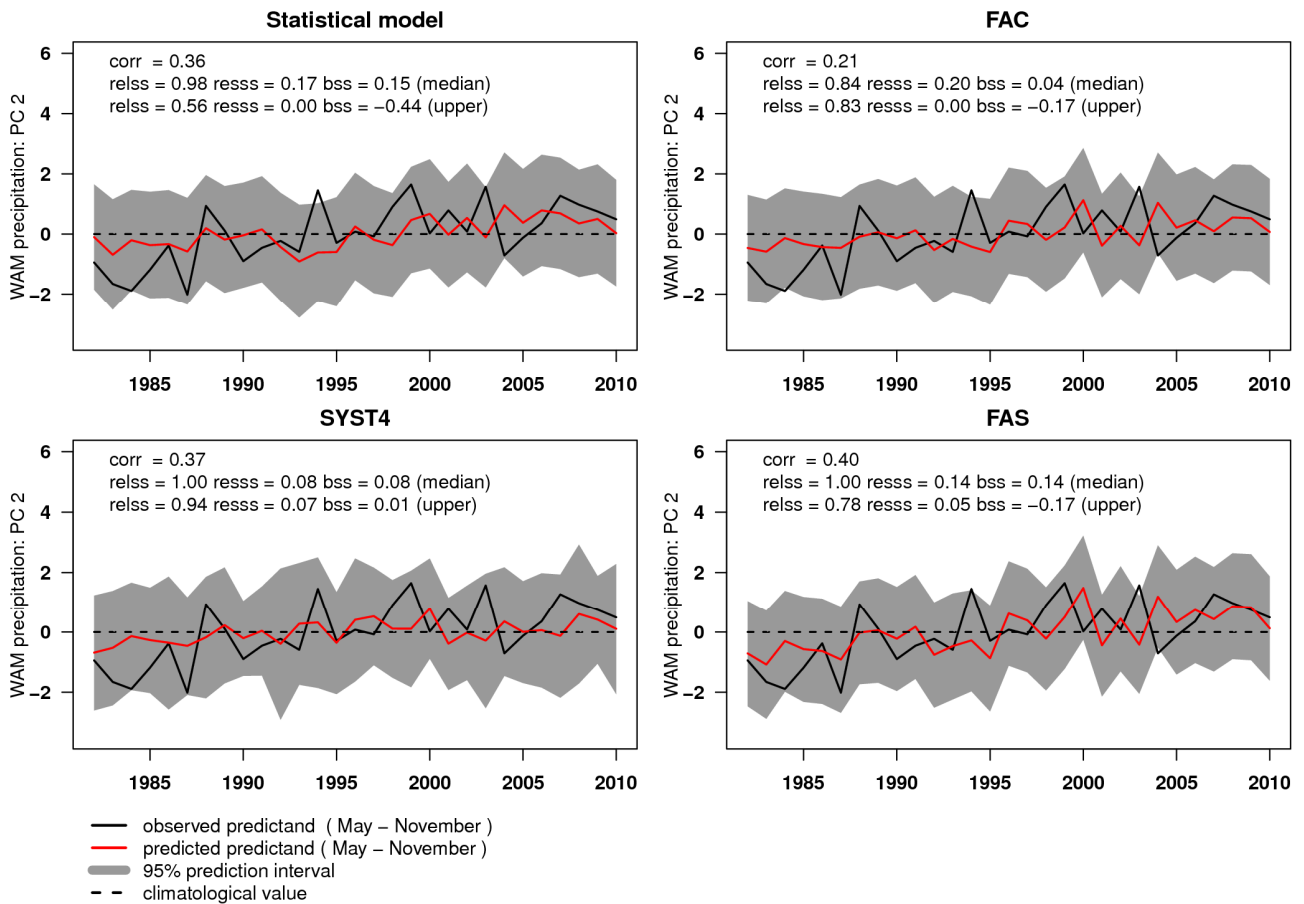


Figure 4. Monthly forecast anomalies of the Sahelian rainfall regime (second EOF mode; PC2) for the Statistical model, SYST4, FAC and FAS. Forecasts are for the start date of November. Observed values (black solid line), predicted values (red solid line), 95% predicted interval (grey area) and the climatology value of November (black dashed line). Several scores are displayed in each panel: the correlation coefficient (corr), and the Brier skill score (bss) and its reliability (relss) and resolution (resss) components for dichotomous events of the PC2 anomalies exceeding the median and the upper quartile

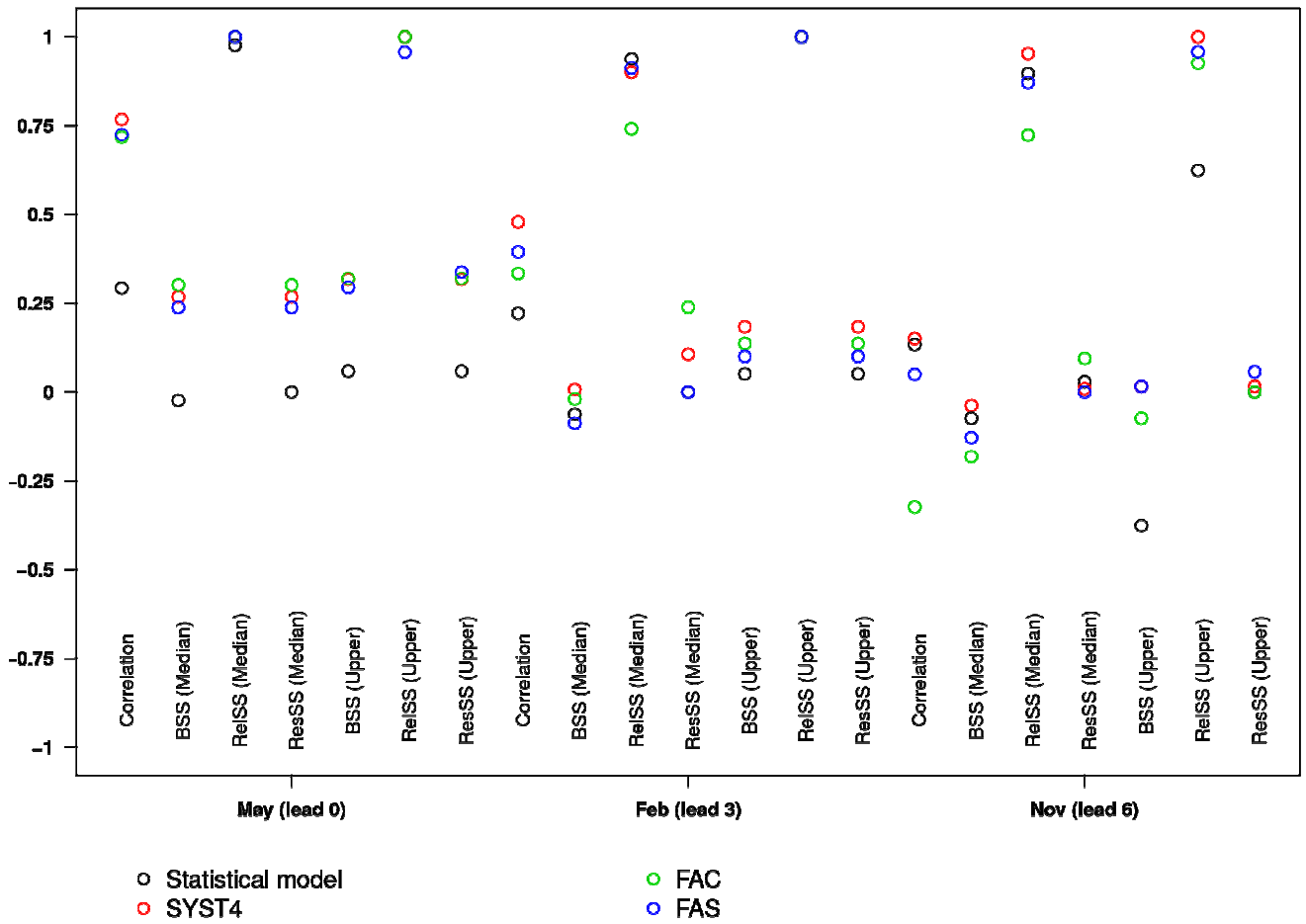


Figure 5. Probabilistic and deterministic forecast quality assessment of the Guinean rainfall regime (first EOF mode; PC1) for the Statistical model (black circle), SYST4 (red circle), FAC (green circle) and FAS (blue circle). Several scores are displayed: the correlation coefficient (correlation), and the Brier skill score (BSS) and its reliability (RelSS) and resolution (ResSS) components for dichotomous events of the PC1 anomalies exceeding the median and the upper quartile.

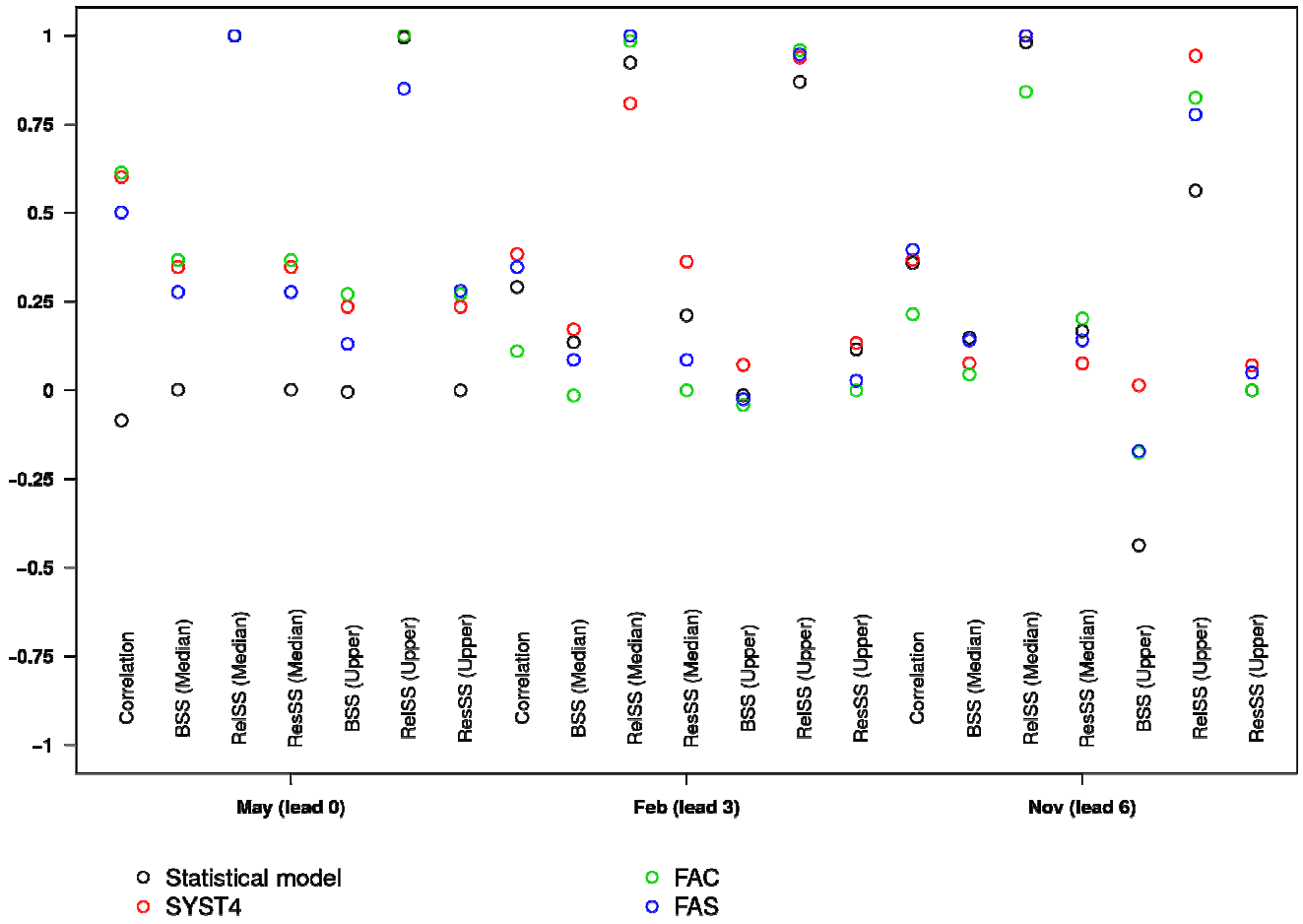


Figure 6. Same as Figure 5, but for the Sahelian rainfall regime (second EOF mode; PC2).